Magnetoconductance in quantum waveguides with inhomogeneous magnetic fields

Ben-Yuan Gu[a)]
Department of Physics, The University of Hong Kong, Pokfulam Road, Hong Kong, China and Institute of Physics, Academia Sinica, P. O. Box 603, Beijing 100080, China

Jian Wang
Department of Physics, The University of Hong Kong, Pokfulam Road, Hong Kong, China

(Received 29 April 1998; accepted for publication 1 November 1998)

We discuss the properties of magnetotransport of electrons in quantum waveguides (QWs) in the presence of laterally inhomogeneous magnetic fields perpendicular to the QW plane. The inhomogeneous magnetic fields can be produced by the deposition, on top of a heterostructure, of ferromagnetic stripes with magnetization perpendicular and parallel to the two-dimensional electron gas. It is found that the magnetoconductance in such a device as a function of the Fermi energy of electrons exhibits square-wave-like oscillations that are strongly dependent on the geometrical arrangement and magnetic configurations in the QWs. Different dispersions can be observed. From analyses of the magnetic effective potential, the dispersion relations can be understood well. In some magnetic modulations, the energy spectrum exhibits a bump superimposed upon every bulk Landau level. It is these oscillatory structures in dispersions that lead to square-wave-like shaped modulation in magnetoconductance, which may serve as an energy filter of electrons. © *1999 American Institute of Physics.* [S0021-8979(99)10603-0]

I. INTRODUCTION

Currently much attention has been focused on the exploration of the properties of electron transport in microstructures created by high mobility GaAs/Al_xGa_{1-x}As heterostructures in a perpendicular magnetic field.[1] In these structures various energy dispersion relations and novel transport behaviors of electrons can be observed. These physical properties offer concepts of new quantum devices. One important low-dimensional device is the quantum waveguide (QW) which can be achieved via field effects on a two-dimensional electron gas (2DEG) system.[2,3] Another important quantum interference device is dual-coupled quantum waveguides. A number of authors have focused on studies of coupled quantum waveguides in zero and finite magnetic fields due to their applications to the electronic waveguide direction coupler.[4–11] Electron transport properties in nonuniform magnetic fields have also attracted much attention and have been under intensive investigation in recent years.[12–23] With the application of spatially inhomogeneous magnetic fields, a number of alternative magnetic structures were proposed on 2DEG,[24–28] such as magnetic superlattices by the patterning of ferromagnetic materials integrated by semiconductors.[24] To date, most investigations are focused, theoretically or experimentally, on the effect of inhomogeneous magnetic fields modulated along the transport (longitudinal) direction of QWs. To our knowledge, the effect of laterally inhomogeneous magnetic fields in QWs still receives little attention.[12–16]

Recently, Müller studied the single-particle electronic structure of a 2DEG in a wide quantum waveguide with an inhomogeneous magnetic field applied.[12] He found that in the presence of a laterally linear varying magnetic field in the interior of the sample the Landau states are no longer stationary but propagate perpendicularly to the field gradient and exhibit a remarkable time-reversal asymmetry. This means that in the presence of such an inhomogeneous magnetic field in the 2DEG, which creates two different magnetic domains, there exist current-carrying states (hereafter referred to as magnetic edge states) near the interface between two domains. These magnetic edge states possess quite different characteristics from conventional ones. Thus, various new phenomena of electron transport in magnetic modulation structures are expected.[14,15]

In previous work,[14] we have theoretically investigated electronic states and magnetotransport properties of QWs in the presence of step-varying magnetic fields. It was found that the magnetoconductance in such a structure as a function of the Fermi energy of electrons exhibits a staircase type variation or square-wave-like shaped oscillations, depending on the specific magnetic configurations in the QWs. The properties of the magnetotransport of electrons are closely related to the magnetic effective potential and energy dispersions in the structures. Only in some three-magnetic-strip structures, do the dispersion relations of magnetic scattering states exhibit oscillation structures superimposed on bulk Landau levels. It is the oscillatory behavior in dispersions that leads to square-wave-like modulation in conductance.

Motivated by this work, the purpose of this article is to provide an extended investigation of electronic states and magnetotransport properties for QWs in the presence of more realistic magnetic fields instead of ideal step-varying fields. Experimentally, inhomogeneous magnetic fields on the nanometer scale can be realized with, for instance, the creation

a)Electronic mail: guby@aphy.iphy.ac.cn; jianwang@hkusub.hku.hk

of magnetic dots,[29] the patterning of ferromagnetic materials,[24] and the deposition of type-II superconducting materials onto heterostructures.[30] More recently, Matulis *et al.*[31] proposed four realistic magnetic barriers produced by the deposition, on top of a heterostructure, of ferromagnetic thin film, or of conducting stripes, or of superconducting plates interrupted by a stripe. The question is raised, What happens to the behavior of the magnetotransport of electrons in QWs under the application of realistic magnetic fields? From our calculations, it was shown that the application of laterally inhomogeneous magnetic fields to QWs can produce various energy dispersions and different patterns of magnetoconductance. The energy dispersions strongly depend on the geometrical and magnetic configurations. For some magnetic modulation structures, the conductance spectrum exhibits well-defined square-wave-like shaped oscillations. In these cases, the energy dispersions present a wide bump superimposed upon each bulk Landau level, leading to square-wave-like oscillations in magnetoconductance. The basic feature of the model device is insensitive to the elimination of small fine structures in the magnetic field distribution. When replacing the realistic field distribution by its average field with the step-varying profile, the main results are essentially preserved.

This article is organized as follows. In Sec. II there is a brief description of the model devices and the necessary formulas used in the calculations. The calculated results are presented in Sec. III with analyses. A brief summary is in Sec. IV.

II. MODEL AND FORMULAS

The system considered is a long narrow quantum waveguide with a width W subject to an inhomogeneous magnetic field perpendicular to the QW lying in the $X-Y$ plane. We choose, for simplicity of calculation, the hard-wall confinement potential for the boundaries. The transverse potential inside the QW is set to zero, i.e.,

$$V_c(y)=\begin{cases}0, & 0\leqslant y\leqslant W,\\ \infty, & \text{otherwise.}\end{cases}$$

The magnetic field is oriented along the $\hat{\mathbf{z}}$ direction. As a prototype, two types of magnetic field modulations are considered here; they may be produced by the deposition, on top of a heterostructure, of a ferromagnetic stripe with magnetization (a) perpendicular and (b) parallel to the 2DEG located at a distance z_0 below the stripe; cf. Figs. 1 (a) and 1(b) in Ref. 31. For these two types of modulations, the corresponding magnetic field distributions in the 2DEG can be expressed by $\mathbf{B}=B(y,z_0)\hat{\mathbf{z}}$,

$$B(y,z_0)=B_0[K(Y+d_0/2,z_0)-K(Y-d_0/2,z_0)], \tag{1}$$

where $Y=y-y_0$, y_0 stands for the y coordinate of the center line of the ferromagnetic stripe; (a) $B_0=M_0h/d_0$, $K(y,z_0)=2yd_0/(y^2+z_0^2)$, and (b) $B_0=M_0h/d_0$, $K(y,z_0)=-z_0d_0/(y^2+z_0^2)$, in which M_0 is the magnetization of the ferromagnetic stripe, and $d_0(h)$ is the thickness (height) of the stripe. It has been assumed here that magnetic stripe is extremely thin, i.e., $h/d_0\ll 1$ and $h/z_0\ll 1$. According to the Landau gauge, the vector potential is $\mathbf{A}=(-A_0(y,z_0),0,0)$ and the magnetic field is given by $B(y,z_0)=dA_0(y,z_0)/dy$. Therefore, the vector potential possesses the following explicit expressions:[27]

$$A_0(y,z_0)=B_0d_0\ln\frac{(Y+d_0/2)^2+z_0^2}{(Y-d_0/2)^2+z_0^2}, \tag{2}$$

$$A_0(y,z_0)=B_0d_0\left[\tan^{-1}\left(\frac{Y-d_0/2}{z_0}\right)-\tan^{-1}\left(\frac{Y+d_0/2}{z_0}\right)\right], \tag{3}$$

for cases (a) and (b), respectively. The wave function of the Schrödinger equation of a single electron for a two-dimensional system can be expressed as

$$\Psi(x,y)=e^{+ik_xx}\psi(y), \tag{4}$$

where $\psi(y)$ satisfies the one-dimensional Schrödinger equation

$$\left\{-\frac{\hbar^2}{2m^*}\frac{d^2}{dy^2}+\frac{\hbar^2}{2m^*}[k_x-eA_0(y)/\hbar c]^2+V_c(y)\right\}\psi(y)=E\psi(y). \tag{5a}$$

Here, $m^*=0.067m_0$ is the electron effective mass for GaAs. The magnetic field enters into the Schrödinger equation as an additional momentum proportional to the vector potential. For the convenience of the following discussions, we introduce the effective potential incorporating the effect of the magnetic field as $V_{\text{eff}}(y)$, and rewrite Eq. (5a) as

$$\left[-\frac{\hbar^2}{2m^*}\frac{d^2}{dy^2}+V_{eff}(y)+V_c(y)\right]\psi(y)=E\psi(y), \tag{5b}$$

where $V_{\text{eff}}(y)$ is given by

$$V_{\text{eff}}(y)=\frac{\hbar^2}{2m^*}[k_x-eA_0(y)/\hbar c]^2. \tag{6a}$$

The total potential is $V(y)=V_{eff}(y)+V_c(y)$. To solve this equation, we expand $\psi(y)$ in terms of a set of complete bases, corresponding to the transverse eigenfunctions of the QW at zero field,

$$\psi(y)=\sum_{j=1}^{N_s}f_j(y)c_j, \tag{7}$$

where

$$f_j(y)=\sqrt{\frac{2}{W}}\sin\left(\frac{\pi j}{W}y\right),$$

and c_j is determined by

$$\sum_{j=1}^{N_s}\left\{\left[\left(\frac{k_FW}{\pi}\right)^2-j^2\right]\delta_{nj}-\langle n|\left[k_x\Big/\left(\frac{\pi}{W}\right)-2A_0(y)W/\phi_0\right]^2|j\rangle\right\}c_j=0, \tag{8}$$

where $k_F^2=2m^*E_F/\hbar^2$, $\phi_0=hc/e$ is the quantum flux, and

$$\langle n|G(y)|j\rangle\equiv\int_0^W f_n(y)G(y)f_j(y)dy.$$

Hereafter we always employ dimensionless quantities. The energy is measured in units of $E_1=(\hbar^2/2m^*)(\pi/W)^2$; the length is measured by W. The effective potential of Eq. (6a) can be written as

$$\tilde{V}_{\rm eff}(y)=V_{\rm eff}(y)/E_1=[\tilde{k}_x-2A_0(y)W/\phi_0]^2, \tag{6b}$$

where $\tilde{k}_x=k_x/(\pi/W)$. It is worth pointing out that this effective potential possesses the following scaling invariance: When $W\rightarrow\alpha W$, $d_0\rightarrow\alpha d_0$, and at the same time $B_0\rightarrow B_0/\alpha^2$, the normalized effective potential remains unchanged. Equation (8) can be solved on an expanded basis.[23,32] For a given Fermi energy E_F, we obtain a set of eigen-wave numbers $\{\pm k_{x,n}\}$ and eigen-wave functions $\{\psi_n^{\pm}(y)\}$.

Assuming that two reservoirs connected to the QW fill all the edge states of electrons below the Fermi energy completely, and that the QW is long enough so that there is no backscattering process related to the end of the QW, then, the magnetoconductance of the structures is given by[33]

$$G(E_F)=(2e^2/h)N_p(E_F), \tag{9}$$

where $N_p(E_F)$ stands for the number of propagating modes with positive group velocity at the Fermi energy E_F. The group velocity of an electron in the propagating mode ψ_α is evaluated with

$$v_\alpha=\frac{\hbar}{m^*}\int_0^W \psi_\alpha^*\left[k_\alpha-\frac{2\pi A_0(y)}{\phi_0}\right]\psi_\alpha(y)dy. \tag{10}$$

III. RESULTS AND ANALYSES

We now calculate the energy spectrum and the magnetoconductance of the system where we have fixed the width of the QW to be $W=2000$ Å. First, we consider a model device in which the 2DEG is subjected to an inhomogeneous magnetic field produced by a ferromagnetic stripe with magnetization perpendicular to the QW plane. The schematic view of the structure is shown in the inset of Fig. 1(a). The 2DEG is located at a distance z_0 below the magnetic stripe. The ferromagnetic stripe is placed at the central position on top of the QW. The separation between the edge of the stripe and the boundary of the QW denotes a_0. We set $a_0=W/4$, $d_0=W/2$, $\tilde{z}_0=z_0/d_0=0.1$, and the maximum of the magnetic field $B_{\rm max}=3$ T. The reduced distribution of the realistic magnetic field is displayed by a solid line in Fig. 1(a). For a comparison, its average field with a stepwise profile is also depicted in Fig. 1(a) by a dashed line. The energy dispersion relation of the electron is displayed in Fig. 1(b). The calculated conductance as a function of the Fermi energy of electrons is plotted in Fig. 1(c).

Considering the structure symmetry of this device, it is expected that the dispersion curves should be symmetric about $\tilde{k}_x=0$ point. It is seen from Fig. 1(b) that the energy spectrum seems to be made up of three groups of dispersion curves. Two groups of dispersion curves demonstrate a semiparabolic nature, and belong to two negative weak field regions in the QW. They form the left and right branches of the dispersions. The central part of the dispersion curves has contributions from positive strong field region, in which

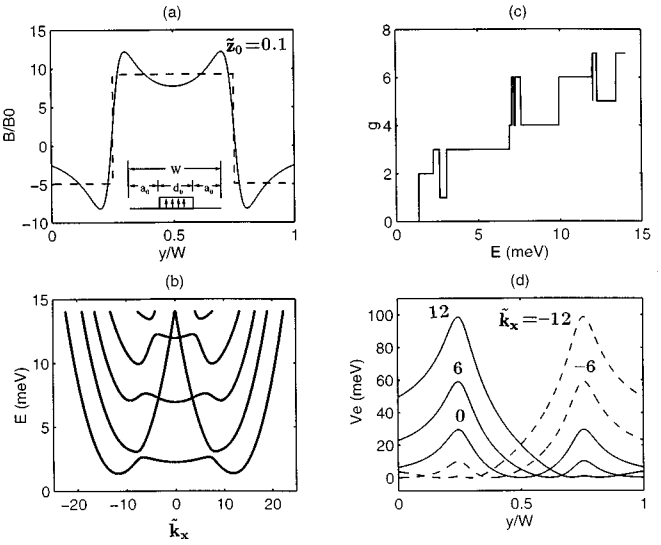

FIG. 1. Results for the QW in the presence of a laterally inhomogeneous magnetic field perpendicular to the QW plane. The magnetic field is produced by the deposition, on top of the QW, of a ferromagnetic stripe with magnetization perpendicular to the QW plane located at a distance z_0 below the stripe. A schematic representation of a model device is shown in the inset of (a). (a) Distribution of the realistic (solid line) and the average (dashed line) magnetic fields. (b) Energy dispersion relations. (c) Calculated conductance (in units of $2e^2/h$) as a function of Fermi energy. (d) Magnetic effective potential. The relevant parameters chosen are QW width $W=2000$ Å, $a_0=W/4$, $d_0=W/2$, $\tilde{z}_0=z_0/d_0=0.1$, and $B_{\rm max}=3$ T.

there exist both bulk Landau levels and magnetic edge states. Owing to the presence of magnetic domains, the strong coupling between magnetic edge states leads to splitting and crossing of the levels, and to substantial distortion of the dispersion curves. The corresponding conductance as a function of the Fermi energy of electrons is displayed in Fig. 1(c). It exhibits basically a square-wave-like pattern consisting of a series of valleys with different widths as well as plateaus with different heights and widths.

To have a better understanding of the character of dispersion curves, we display a profile of the magnetic effective potential $V_{\rm eff}(y)$ for several $\tilde{k}_x$ in Fig. 1(d). It is clearly seen that the profile of the effective potential achieves space-reversal symmetry with respect to the center line of the QW when the sign of $\tilde{k}_x$ is reversed. For the finite values of $|\tilde{k}_x|$, all the effective potentials exhibit barrier-well structures. The total potential seems to be an infinite depth quantum well with a parabolic-shaped bottom. A series of quantization levels survived in these quantum subwells. When $\tilde{k}_x\sim 0$, the effective parabolic well is located at the center of the sample. The structure of the bulk Landau levels dominates. Thus the nearly flat plateaus around $\tilde{k}_x\sim 0$ emerge in the dispersions. Note that the shape of the plateaus behaves slightly concave, just corresponding to the concave varying tendency in the magnetic field distribution in the central region of the QW.

Roughly speaking, this model device is quite similar to the QW with a three-magnetic-strip-modulation structure that was discussed in Ref. 14 (cf. Fig. 6 in Ref. 14). In order to present a detailed comparison of the character of the QW under application of the realistic magnetic field and its average field with a stepwise profile, we prefer to demonstrate

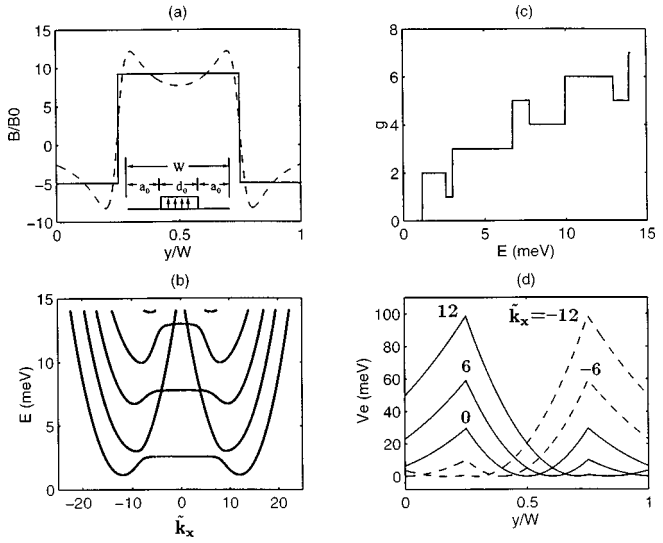

FIG. 2. Same as Fig. 1 except for the magnetic field distribution taking an average field with a step-varying version (solid line).

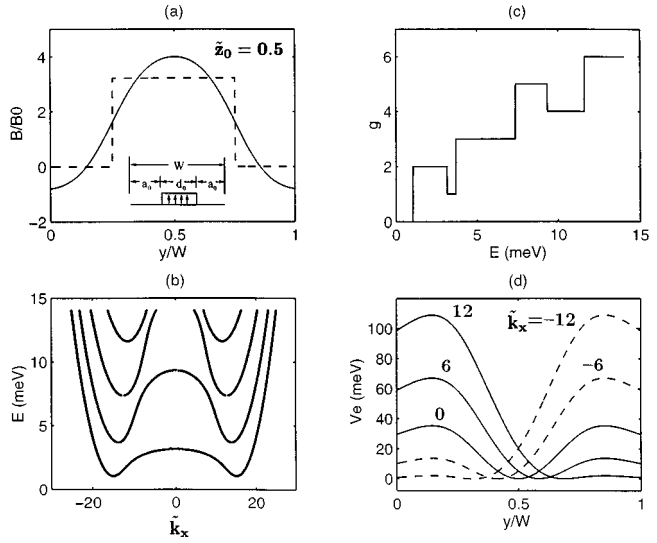

FIG. 3. Same as Fig. 1 except for $\tilde{z}_0 = z_0 / d_0 = 0.5$.

numerical results in the QW subjected to an average stepwise varying field which is shown by a solid line in Fig. 2(a). The corresponding dispersion curves, the calculated conductance spectrum, and the magnetic effective potential are demonstrated in Figs. 2(b)–2(d), respectively. Comparing them with their analogs in Fig. 1, it is evident that they exhibit similar patterns, with little difference. For instance, the Landau plateaus in the dispersions become quite flat. The conductance behavior in the average field case exhibits well-defined square-wave-like oscillations compared with Fig. 1(c). From a global point of view, we can safely say that the essential character of the QW is basically retained when the realistic magnetic field is replaced by its average stepwise field.

The particular distribution of the magnetic field produced by the ferromagnetic stripe depends on the distance z_0. We now reveal the characteristic of the QW by changing the distance to $\tilde{z}_0 = 0.5$. All the other parameters remain the same as those in Fig. 1. The profile of the realistic (average) magnetic field is shown in Fig. 3(a) by a solid (dashed) curve. It is evident that the profile of the magnetic field exhibits a sinusoidal function form. The corresponding energy dispersions, the conductance spectrum, and the magnetic effective potential are depicted in Figs. 3(b)–3(d), respectively. It is clearly seen from Fig. 3(b) that the dispersions are composed of three groups of dispersion curves. The left (right) branch has contributions from the negative weak magnetic field region around $y/W = 0$ $(y/W = 1)$, and exhibits a parabolic shape in the dispersions. However, the middle of the dispersions is ascribed to the contribution from a positive strong field region around $y/W = 0.5$ [see Fig. 3(a)], existing at bulk Landau levels. The dispersions are symmetric due to the symmetry of the magnetic field distribution in the sample. Since the strength of the magnetic field in the middle region is larger than that in the other two regions near the boundaries, the subbands in the middle region lift up. Finally, bumps are formed and superimposed on the bulk Landau levels in the central region in $\tilde{k}_x$ space. At the same time, distinct minigaps are created. The dispersions display oscillatory structures. When scanning the Fermi energy, it is these bumps and minigaps that lead to the well-defined square-wave-like shaped oscillations in the conductance spectrum, seen in Fig. 3(c).

To provide a good explanation of the behavior of the dispersions, we present the calculated magnetic effective potential in Fig. 3(d). It is clearly seen that the potential performs space-reversal symmetry mapping with respect to the center line of the model device if the sign of $\tilde{k}_x$ is reversed. When $\tilde{k}_x = 0$, V_{eff} exhibits a nearly parabolic-potential well form with a finite depth. Consequently, a series of bulk Landau levels are produced. Note that the bumps superimposed on the bulk Landau plateaus almost correspond to the maximum of the cosine-like function of the magnetic field distribution. As $|\tilde{k}_x|$ increases from zero, the shape of parabolic-potential well is substantially distorted. When $|\tilde{k}_x|$ is much larger, the total potential behaves like an infinite-depth triangular well declined to the boundary wall. Thus the boundary states dominate the property of the transport of electrons and they decide the profiles of the rightmost and leftmost branches in the dispersions.

Notice in Fig. 3(d) the difference in the magnetic effective potentials for electrons moving in the positive k_x direction and electrons moving in the negative k_x direction. For large $|\tilde{k}_x|$ the effective potential behaves like a semi-parabolic potential. The minima of the potentials are located at different positions in space for $k_x > 0$ and $k_x < 0$ propagating modes, and consequently the maxima of electron probability densities appear in different spatial positions in the QW. Electrons with positive k_x are confined in the right-half region of the QW and electrons with negative k_x are confined in the left-half region of the QW. It is therefore not surprising that electrons in such a QW will propagate along different boundaries.

Also in order to provide a detailed comparison of the characteristics of the model device after replacing the realistic field by its average field with a stepwise shape, we dis-

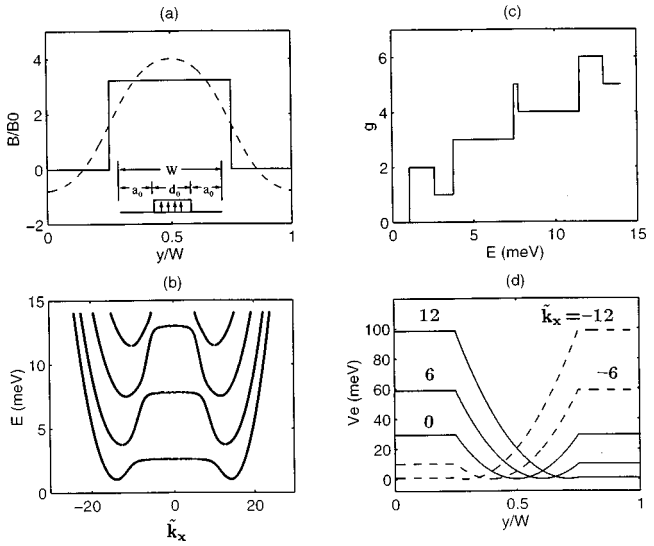

FIG. 4. Same as Fig. 3 except for the magnetic field distribution taking an average field with a stepwise-varying profile (solid line).

play the results in Fig. 4. Comparing them with their analogs in Fig. 3, it is found that this replacement influences the performance of the device only slightly less.

We now envisage the feature of the QWs subjected to an inhomogeneous magnetic field with a different version. The magnetic field is produced by a ferromagnetic stripe with magnetization parallel to the QW plane; the 2DEG is located at a distance z_0 below the stripe. A sketch of the structure is shown in the inset of Fig. 5(a). We place the stripe attached to the right-boundary wall of the QW. The separation between the left edge of the stripe and the left-boundary wall denotes a_0. The parameters are $W=2000$ Å, $a_0=W/2$, $d_0=W/2$, $\tilde{z}_0=z_0/d_0=0.1$ or 0.5, and $B_{\max}=5$ T. The distributions of fields are illustrated in Figs. 5(a) and 6(a) for $\tilde{z}_0=0.1$ and $\tilde{z}_0=0.5$, respectively. The corresponding energy dispersions are shown in Figs. 5(b) and 6(b), respectively. The calculated conductance spectra are displayed in Figs. 5(c) and 6(c) and the magnetic effective potentials are depicted in Figs. 5(d) and 6(d), respectively. Both the conductance spectra behave like square-wave oscillations. The conductance spectrum in Fig. 6(c) exhibits a more regular pattern than that in Fig. 5(c) owing to a smoother variation of the magnetic field distribution [see Fig. 6(a)]. The conductance spectrum behaves like regular square-wave-like shaped oscillations, and the sharp peak structures disappear completely. The origin of the conductance oscillations can be explained by similar discussions to those mentioned above.

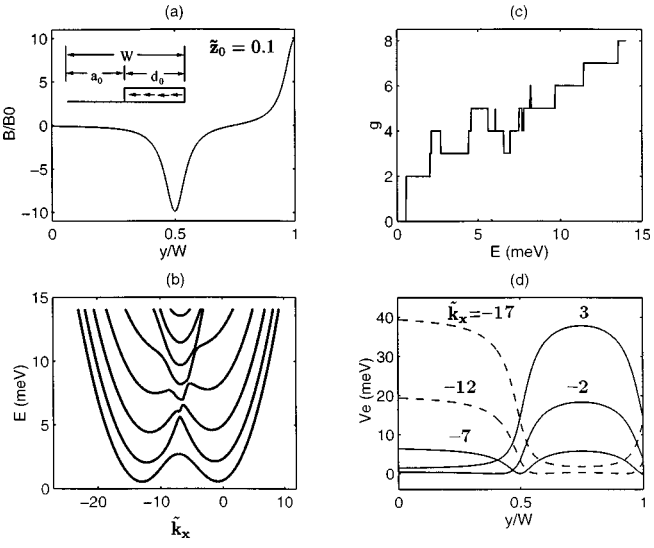

FIG. 5. Results for the QW in the presence of a laterally inhomogeneous magnetic field, which is created by a ferromagnetic stripe with magnetization parallel to the QW plane located at a distance z_0 below the stripe. A sketch of the structure is displayed in the inset of (a). (a) Distribution of the realistic magnetic field. (b) Energy dispersion relations. (c) Calculated conductance (in units of $2e^2/h$) as a function of Fermi energy. (d) Magnetic effective potential. The relevant parameters are $W=2000$ Å, $a_0=W/2$, $d_0=W/2$, $\tilde{z}_0=z_0/d_0=0.1$, and $B_{\max}=5$ T.

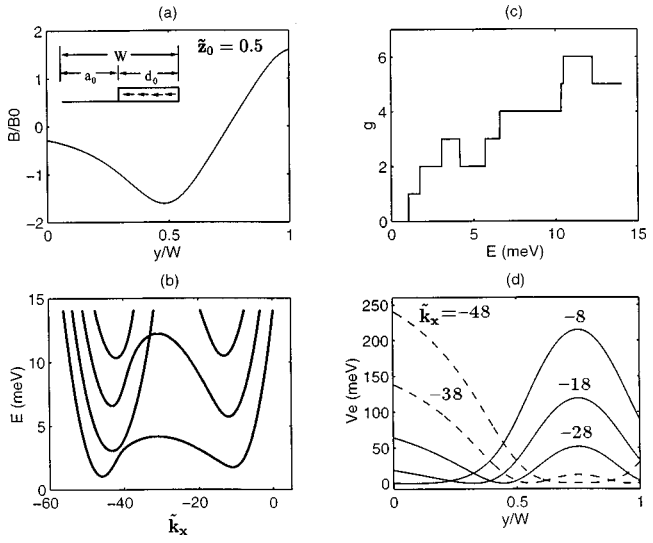

FIG. 6. Same as Fig. 5 except for $\tilde{z}_0=0.5$.

It is worth emphasizing the fact that the particular patterns of the spectra strongly depend on the geometric structures and magnetic modulations. When changing these factors, various patterns can be observed. For instance, in case (b), when $a_0=0$, $d_0=W$, and $\tilde{z}_0=0.1$ or when placing the magnetic stripe on the central position of the QW, with $d_0=W/3$, $a_0=W/3$, and $\tilde{z}_0=0.1$, the conductance spectrum exhibits a trivial staircase version.

IV. SUMMARY

We have revealed transport properties of electrons in QWs subjected to a realistic inhomogeneous magnetic field. We considered two types of magnetic field modulations, which may be achieved by the deposition, on top of a heterostructure, of ferromagnetic stripes with magnetization (a) perpendicular and (b) parallel to the 2DEG. It is found that the magnetoconductance spectra in such devices exhibit square-wave-like shaped oscillations, strongly dependent on the geometrical structures and the particular distribution of the magnetic fields in the QWs. To understand the origin of the oscillatory magnetoconductance spectra, we have calculated the energy dispersion relations of electrons in propagat-

ing states and the corresponding magnetic effective potential. Due to the effect of the magnetic effective potential, for some magnetic modulation structures, the corresponding dispersions are composed of a bump superimposed on every bulk Landau level, forming oscillation structures and minigaps. It leads to the square-wave-like conductance spectrum. From a global point of view of the characteristics of the devices, the replacement of the realistic field by its average field with a step-varying profile has little influence. A new way of artificially tailoring the conductance spectrum is proposed by introducing the lateral modulations of magnetic fields.

Finally, we would like to comment on the possibility of realizing, experimentally, the model devices we have studied in this article. Inhomogeneous magnetic fields on the nanometer scale can be established with the use of several methods.[24–26,29–31] For our model devices, lateral inhomogeneous magnetic fields may be produced with a stripe of ferromagnetic thin film deposited on a heterostructure[24–26] or through the integration of lithgraphically patterned superconducting materials on the top of the heterostructures.[30,31] Producing the ideal magnetoconductance spectrum with a well-defined-square-wave-like shaped pattern requires an appropriate high field. For instance, in the sample shown in Fig. 1(a), the magnetization of the ferromagnetic stripe is required to be $M_0 = B_0 d_0/h = (B_{\max}/12.196)(d_0/h) = 0.246(d_0/h)T$ when $B_{\max} = 3$ T. If we set $h/d_0 = 0.2$, then $M_0 = 1.23$ T. Of course, this magnetization value still is too large in practice. However, we have indicated in Sec. II that the pattern of the magnetoconductance spectrum is essentially decided by the magnetic effective potential given in Eq. (6b), and this effective potential possesses the following scaling invariance. When $W \to \alpha W$, $d_0 \to \alpha d_0$, and at the same time $B_0 \to B_0/\alpha^2$, the normalized effective potential remains invariant. Therefore, we may employ a ferromagnetic stripe of large thickness to reduce its necessary magnetization to match practical fabrication.

ACKNOWLEDGMENTS

The authors gratefully acknowledge the financial support by a RGC grant from the SAR government of Hong Kong under Grant No. HKU 7112/97P, a CRCG grant from The University of Hong Kong, and a research grant from the Chinese National Science Foundation. They also thank the Computer Center of The University of Hong Kong for computational facilities.

[1] C. W. J. Beenakker and H. van Houton, in *Solid State Physics: Semiconductor Heterostructures and Nanostructures*, edited by H. Ehrenreich and D. Turnbull (Academic, New York, 1991), Vol. 44, p. 1, and references cited therein.

[2] B. J. van Wees, H. van Houton, C. W. J. Beenakker, J. G. Williamson, L. P. Kouwenhoven, D. van der Marel, and C. T. Foxon, Phys. Rev. Lett. **60**, 848 (1988); G. Bernstein and D. K. Ferry, J. Vac. Sci. Technol. B **5**, 964 (1987).

[3] F. Sols, M. Macucci, U. Ravaioli, and K. Hess, J. Appl. Phys. **66**, 3893 (1989).

[4] J. A. del Alamo and C. C. Eugster, Appl. Phys. Lett. **56**, 78 (1990).

[5] C. C. Eugster, J. A. del Alamo, M. J. Rooks, M. R. Melloch, Appl. Phys. Lett. **60**, 642 (1992); Phys. Rev. B **46**, 10146 (1992); *ibid.* **48**, 15057 (1993); Phys. Rev. Lett. **67**, 3586 (1991).

[6] R. Q. Yang and J. M. Xu, Phys. Rev. B **43**, 1699 (1991).

[7] J. Q. Wang, S. Q. Yuan, B. Y. Gu, and G. Z. Yang, Phys. Rev. B **44**, 13618 (1991).

[8] J. Q. Wang, B. Y. Gu, and G. Z. Yang, J. Appl. Phys. **72**, 2299 (1992); Phys. Rev. B **47**, 13442 (1993).

[9] Y. Takagaki and K. Ploog, Phys. Rev. B **49**, 1782 (1994).

[10] J. Wang, H. Guo, and R. Harris, Appl. Phys. Lett. **59**, 3075 (1991).

[11] J. Wang, Y. J. Wang, and H. Guo, Phys. Rev. B **46**, 2420 (1992); **47**, 4348 (1993).

[12] J. E. Müller, Phys. Rev. Lett. **68**, 385 (1992).

[13] D. B. Chklovskii, Phys. Rev. B **51**, 9895 (1995).

[14] B. Y. Gu, W. D. Sheng, X. H. Wang, and J. Wang, Phys. Rev. B **56**, 13434 (1997).

[15] H. S. Sim, K. H. Ahn, K. J. Chang, G. Ihm, N. Kim, and S. J. Lee, Phys. Rev. Lett. **80**, 1501 (1998).

[16] I. S. Ibrahim, V. A. Schweigert, and F. M. Peeters, Phys. Rev. B **56**, 7508 (1977); Superlattices Microstruct. **22**, 203 (1997).

[17] B. L. Altshuler and L. B. Ioffe, Phys. Rev. Lett. **69**, 2979 (1992); T. Sugiyama and N. Nagoasa, *ibid.* **70**, 1980 (1993); S.-C. Zhang and D. P. Arovas, *ibid.* **72**, 1886 (1994).

[18] Z. L. Ji and D. W. L. Sprung, Phys. Rev. B **54**, 8044 (1996); **56**, 1045 (1997).

[19] Y. Takagaki and K. Ploog, Phys. Rev. B **51**, 7017 (1995); **53**, 3885 (1996).

[20] H. Xu, Phys. Rev. B **52**, 5803 (1995).

[21] X. Q. Li and F. M. Peeters, Superlattices Microstruct. **22**, 243 (1997); X. Q. Li, F. M. Peeters, and A. K. Geim, J. Phys.: Condens. Matter **9**, 8065 (1997).

[22] C. S. Kim and O. Olendski, Phys. Rev. B **53**, 12917 (1996).

[23] H. Tamura and T. Ando, Phys. Rev. B **44**, 1792 (1991).

[24] M. L. Leadbeater, S. J. Allen, Jr., F. DeRosa, J. P. Harbison, T. Sands, R. Ramesh, L. T. Florez, and V. G. Keramidas, J. Appl. Phys. **69**, 4689 (1991); K. M. Krishnan, Appl. Phys. Lett. **61**, 2365 (1992); R. Yagi and Y. Iye, J. Phys. Soc. Jpn. **62**, 1279 (1993); M. L. Leadbeater, C. L. Foden, T. M. Burke, J. H. Burroughes, M. P. Grimshaw, D. A. Ritchie, L. L. Wang, and M. Pepper, J. Phys.: Condens. Matter **7**, L307 (1995).

[25] B. T. Jonker, K. H. Walker, E. Kisher, G. A. Prinz, and C. Carbone, Phys. Rev. Lett. **57**, 142 (1986).

[26] I. S. Ibrahim and F. M. Peeters, Am. J. Phys. **63**, 171 (1995); Phys. Rev. B **52**, 17321 (1995).

[27] J. Q. You and L. Zhang, Phys. Rev. B **54**, 1526 (1996); J. Q. You, L. Zhang, and P. K. Ghosh, *ibid.* **52**, 17243 (1995).

[28] Y. M. Mu, Y. Fu, and M. Willander, Superlattices Microstruct. **22**, 135 (1997).

[29] M. A. McCord and D. D. Awschalom, Appl. Phys. Lett. **57**, 2153 (1990).

[30] S. J. Bending, K. von Klitzing, and K. Ploog, Phys. Rev. Lett. **65**, 1060 (1990).

[31] A. Matulis, F. M. Peeters, and P. Vasilopoulos, Phys. Rev. Lett. **72**, 1518 (1994).

[32] S. Chaudhuri and S. Bandyopadhyyay, J. Appl. Phys. **71**, 3027 (1992).

[33] M. Büttiker, Phys. Rev. B **38**, 9375 (1988).